Journal of Physics: Conference Series 2340 (2022) 012022 doi:10.1088/1742-6596/2340/1/012022

Thermodynamical properties of hot and magnetized quark matter within the SU(2) Polyakov-Nambu-Jona-Lasinio model: vacuum magnetic regularization scheme

Sidney S. Avancini[1], **Ricardo L. S. Farias**[2], **Marcus B. Pinto**[1], **William R. Tavares**[1] **and Tulio E. Restrepo**[3]

[1] Departamento de Física, Universidade Federal de Santa Catarina, Florianópolis, SC 88040-900, Brazil

[2] Departamento de Física, Universidade Federal de Santa Maria, Santa Maria, RS 97105-900, Brazil

[3] Instituto de Física, Universidade Federal do Rio de Janeiro, Rio de Janeiro 21941-972, Brazil

E-mail: sidney.avancini@ufsc.br[1], ricardo.farias@ufsm.br[2], marcus.benghi@ufsc.br[1], william.tavares@posgrad.ufsc.br[1], tulioeduardo@pos.if.ufrj.br[3]

Abstract. In this work we implement the recent proposed vacuum magnetic regularization (VMR) scheme to the two flavor Polyakov–Nambu–Jona-Lasinio model in order to describe some basic thermodynamic properties such as the pressure, entropy and energy density. We show that this procedure allows the evaluation of the renormalized magnetization, which agrees with LQCD data. Potential physical differences are also explored when other three possible regularization schemes are adopted to describe the chiral condensate.

1. Introduction

It is well known that the magnetic field independent regularization (MFIR) scheme applied to the SU(2) Nambu–Jona-Lasinio model (SU(2) NJL) can avoid nonphysical behavior in the quark condensate [1] at zero density and temperature. The merit of this procedure is the complete separation of vacuum and magnetic contributions in the gap equation, thermodynamical potential and the random phase approximation (RPA) evaluation of the meson masses. The vacuum magnetic regularization (VMR) scheme includes exact terms of order $\mathcal{O}(eB^2)$ in the effective potential which are usually ignored in the MFIR procedure, since they are mass independent and does not change the phase diagram analysis [2]. On the other hand, the temperature effects bring the possibility to regulate or not the thermal contributions with an ultraviolet cutoff, Λ, which quantitatively shows different behavior at the high temperature even if we consider a scenario with $eB = 0$.

In the present work, we explore the thermodynamical properties in the SU(2) Polyakov–Nambu–Jona-Lasinio, as the pressure, entropy and energy density through four different regularization prescriptions: the thermo-regulated proper-time (TRPT) and standard proper-time (SPT) schemes, which are both non-MFIR procedures with and without an ultraviolet cutoff regularization in the thermal contributions respectively. The remaining regularizations are the MFIR and VMR procedures without regulating the thermodynamical integrals. In order to emphasize one of the advantages of the VMR scheme, we also show that the renormalized magnetization defined in lattice QCD can be obtained.

2. The PNJL at finite magnetic fields

Let us first write the PNJL Lagrangian which is given by [3]

$$\mathcal{L}_{PNJL} = \bar{\psi}\left(i\gamma_\mu D^\mu - \hat{m}_c\right)\psi + G\left[\left(\bar{\psi}\psi\right)^2 + \left(\bar{\psi}i\gamma_5\boldsymbol{\tau}\psi\right)^2\right] - \mathcal{U}\left(\Phi, \bar{\Phi}, T\right) - \frac{1}{4}F^{\mu\nu}F_{\mu\nu}, \quad (1)$$

where ψ are the fermionic fields, τ the isospin Pauli matrices, $\hat{m}_c$ are the current quark masses which, we set as $m_u = m_d \equiv m_c$ while G represents the coupling constant. The covariant derivative is given by $D^\mu = \partial^\mu - iq_f A^\mu_{EM} - iA^\mu$, where q_f represents the quark electric charge ($q_u = 2e/3, q_d = -e/3$), A^μ_{EM} is the electromagnetic gauge field, $F^{\mu\nu} = \partial^\mu A^\mu_{EM} - \partial^\nu A^\nu_{EM}$ where $A^\mu_{EM} = \delta_{\mu 2} x_1 B$ and $\vec{B} = B\hat{e}_3$ within the Landau gauge adopted here. We also consider the Polyakov gauge where the gluonic term, $A^\mu = gA^\mu_a(x)\frac{\lambda_a}{2}$, which only contributes with the spatial components: $A^\mu = \delta^0_\mu A^0 = -i\delta^0_\mu A^4$ where g is the strong coupling, $A^\mu_a(x)$ represents the SU(3) gauge fields while λ_a are the Gell-Mann matrices. The Polyakov potential, $\mathcal{U}\left(\Phi, \bar{\Phi}, T\right)$, is fixed to reproduce pure-gauge LQCD results [4]. For vanishing chemical potential ($\mu = 0$) one has for the expected value of the Polyakov loop $\bar{\Phi} = \Phi$ so that the ansatz proposed in Ref. [5] reads

$$\frac{\mathcal{U}(\Phi, T)}{T^4} = -\frac{1}{2}b_2(T)\Phi^2 + b_4(T)\ln\left[1 - 6\Phi^2 + 8\Phi^3 - 3\Phi^4\right], \quad (2)$$

with

$$b_2(T) = a_0 + a_1\left(\frac{T_0}{T}\right) + a_2\left(\frac{T_0}{T}\right)^2, \quad b_4(T) = b_4\left(\frac{T_0}{T}\right)^3, \quad (3)$$

and the parameters are given in table 1

a_0	a_1	a_2	b_4
3.51	-2.47	15.22	-1.75

Table 1. Parameter set used for the Polyakov loop potential.

3. Regularization prescriptions

In the next subsections we will apply the basic regularization prescriptions for the thermodynamical potential, $\Omega(M, \Phi, T, B)$, of the PNJL SU(2) model.

3.1. The TRPT and SPT frameworks for the thermodynamical potential

The basic structure of the thermodynamical potential in the proper-time representation is given by

$$\Omega(M, \Phi, T, B) = \mathcal{U}(\Phi, T) + \frac{(M - m_c)^2}{4G} + \frac{N_c}{8\pi^2}\sum_{f=u,d}(|q_f|B)^2\int_{\frac{|q_f|B}{\Lambda^2}}^\infty \frac{ds}{s^2}e^{-\frac{M^2 s}{|q_f|B}}\coth(s)$$
$$+ \sum_{f=u,d}\frac{(|q_f|B)^2}{8\pi^2}\int_{\lambda_B}^\infty \frac{ds}{s^2}e^{-\frac{M^2 s}{|q_f|B}}\coth(s)\left\{2\sum_{n=1}^\infty e^{-\frac{|q_f|Bn^2}{4sT^2}}(-1)^n\left[2\cos\left(n\cos^{-1}\frac{3\Phi - 1}{2}\right) + 1\right]\right\}, \quad (4)$$

where the gap equations are given by $\partial\Omega/\partial M|_{\Phi,T} = \partial\Omega/\partial\Phi|_{M,T} = 0$, and should be solved simultaneously. The parameter $\lambda_B = |q_f|B/\Lambda^2$ in the thermomagnetic contribution will define if we are in the TRPT scheme in which we have $\lambda_B \neq 0$ or the SPT scheme where $\lambda_B = 0$, while Λ represents an ultraviolet cutoff of the theory.

3.2. The MFIR and VMR frameworks for the thermodynamical potential

The MFIR scheme is based on the subtraction of magnetic field dependent divergences [6], which, in the PT regularization, is given by

$$\Omega_{MFIR}(M,\Phi,T,B) = \mathcal{U}(\Phi,T) + \frac{(M-m_c)^2}{4G} + \frac{N_c N_f}{8\pi^2}\int_{\frac{1}{\Lambda^2}}^{\infty}\frac{ds}{s^3}e^{-M^2 s}$$
$$-N_c \sum_{f=u,d}\frac{(|q_f|B)^2}{2\pi^2}\left[\zeta'(-1,x_f) - \frac{1}{2}\left[x_f^2 - x_f\right]\ln x_f + \frac{x_f^2}{4}\right]$$
$$+\sum_{f=u,d}\frac{(|q_f|B)^2}{8\pi^2}\int_0^{\infty}\frac{ds}{s^2}e^{-\frac{M^2 s}{|q_f|B}}\coth(s)\left\{2\sum_{n=1}^{\infty}e^{-\frac{|q_f|Bn^2}{4sT^2}}(-1)^n\left[2\cos\left(n\cos^{-1}\frac{3\Phi-1}{2}\right)+1\right]\right\}. \quad (5)$$

The details of the MFIR procedure applied to the PNJL model can be seen in Ref. [2]. The VMR scheme includes a contribution for the thermodynamical potential of order $\mathcal{O}(eB^2)$ which is usually ignored in the MFIR procedure. The thermodynamical potential in the VMR scheme can be written as follows

$$\Omega_{VMR}(M,\Phi,T,B) = \Omega_{MFIR}(M,\Phi,T,B) + \frac{N_c}{24\pi^2}\sum_{q_f=u,d}(|q_f|B)^2\left[\ln\left(\frac{\Lambda^2}{2|q_f|B}\right) + 1 - \gamma_E\right], \quad (6)$$

the gap equation in both procedures are the same and the main differences are present in thermodynamical properties.

4. Results

The thermodynamical properties in which we are interested are the pressure, $P = -\Omega$, the entropy density, $S = \partial P/\partial T$ and the energy density $\mathcal{E} = -P + ST + \mathcal{M}B$, where $\mathcal{M} = \partial P/\partial(eB)$ represents the magnetization. The parameters of the model are chosen to be the same as used in Refs. [2, 7], where $\Lambda = 675$ MeV, $m_c = 3.5$ MeV and the magnetic field dependent coupling $G \equiv G(eB)$ is fitted in order to obtain the effective quark masses calculated in LQCD of ref. [7] and this behavior of $G(eB)$ turns out to reproduce inverse magnetic catalysis [7, 8]. The values of $G(eB)\Lambda^2$ for all regularization prescriptions considered in this work are given in Table 2.

eB [GeV^2]	VMR and MFIR	SPT and TRPT
0.0	5.83200	5.83200
0.2	5.05349	5.19413
0.4	3.74477	4.05506
0.6	2.69719	3.05269

Table 2. The values of $G(eB)\Lambda^2$ for all regularization prescriptions considered.

In Fig. 1 we see the reduced pressure, $\Delta P = P(M,\Phi,B,T) - P(M_0,0,B,0)$ with $M_0 \equiv M(B,T=0)$, the entropy density and energy density for MFIR and VMR schemes. The

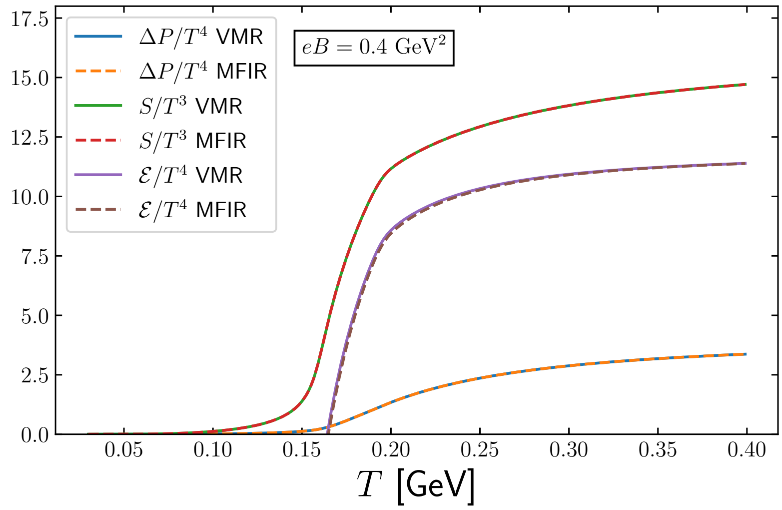

Figure 1. The reduced pressure, entropy density and energy density as function of the temperature for $eB = 0.4$ GeV^2 for VMR and MFIR schemes.

results are almost the same when we compare both regularization for all quantities. The strong magnetic field $eB = 0.4$ GeV^2 was chosen in order to observe possible effects of the regularization in the thermodynamical quantities, which are a little more evident in the energy density. The VMR scheme, in this way, not just reproduce the expected behavior of the MFIR scheme in thermodynamical quantities, but also allows us to explore more quantities, as the renormalized magnetization [2, 9].

In Fig.2 we see the normalized chiral condensate as a function of the magnetic field for all regularization procedures at $T = 250$ MeV. We observe the magnetic catalysis for the MFIR, VMR and SPT schemes. An inverse catalysis is observed for TRPT scheme, which shows that the entanglement between vacuum and magnetic contributions and an ultraviolet cutoff in the thermal contributions have physical consequences.

We also present the renormalized magnetization, $\mathcal{M}^r$, in Fig. 3 as a function of the magnetic field at $T = 0$ in the SU(2) PNJL model in order to compare with lattice QCD [10]. This is possible once we adopt the following approach

$$\mathcal{M}^r \cdot eB = \mathcal{M} \cdot eB - (eB)^2 \lim_{eB \to 0} \frac{\mathcal{M} \cdot eB}{(eB)^2}\bigg|_{T=0}, \tag{7}$$

in which we have applied the same idea developed in [10] to the SU(2) PNJL. This is possible through the VMR scheme that enables us to mimic the renormalized magnetization in the model. In the calculation of the renormalized magnetization we have adopted a fixed coupling $G \equiv G(eB = 0)$, in order to avoid physical complications associated with removing extra $\mathcal{O}(eB^2)$ contributions. An interesting and more detailed discussion can be seen in [2, 9].

5. Conclusions

In this work we have analyzed the role of different regularization prescriptions in the context of the hot and magnetized SU(2) PNJL model. The MFIR scheme is applied to the thermodynamical potential in order to full separate the magnetic and vacuum contributions while the VMR scheme recovers mass independent terms that are avoided in the former. These two procedures, in general, can give very similar results, but when considering the VMR scheme

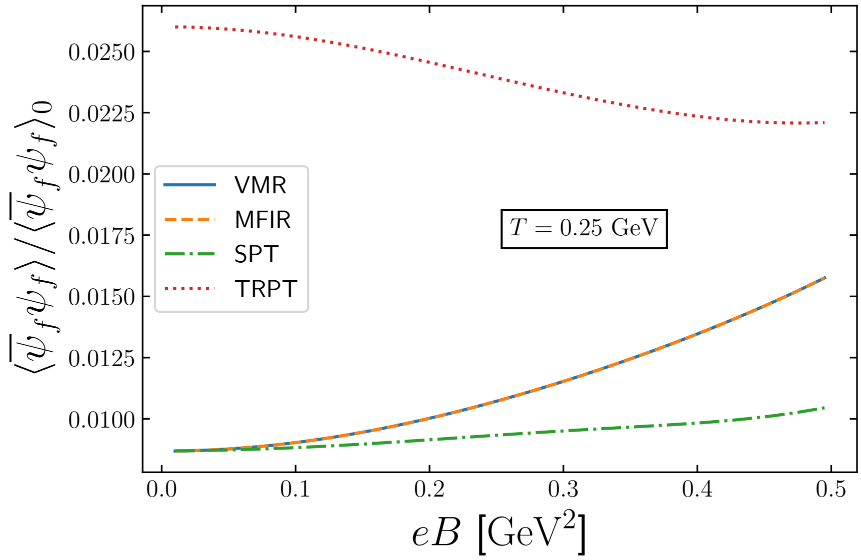

Figure 2. The normalized chiral condensate as function of the magnetic field at $T = 250$ MeV for all regularization prescriptions adopted in this work.

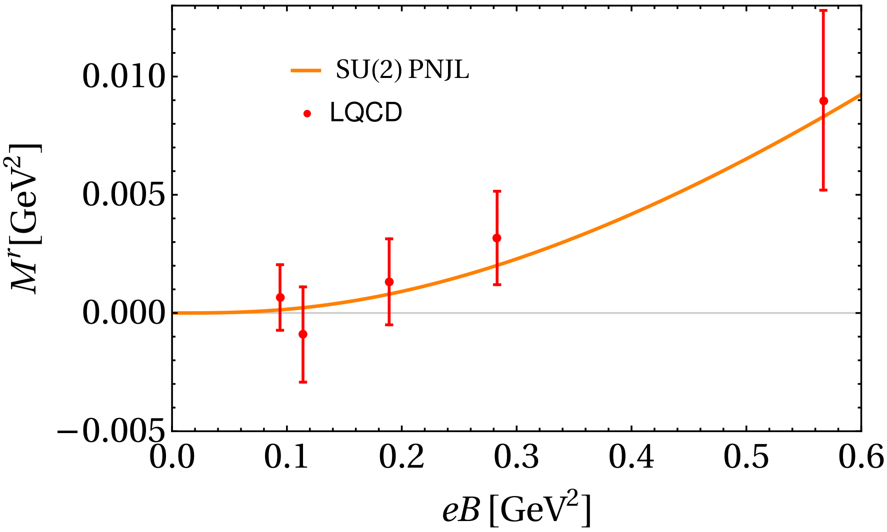

Figure 3. The renormalized magnetization in the SU(2) PNJL model with $G \equiv G(B = 0)$ at $T = 0$ compared with LQCD data from Ref. [10].

we are able to explore more quantities as the renormalized magnetization.

The TRPT and SPT schemes are both non-MFIR schemes in which one can consider or not an ultraviolet cutoff in the thermal integrals respectively. Previous works show that regulating the thermal contributions can change abruptly the Stefan-Boltzmann limit in the pressure and sound velocity. The present manuscript also shows that the TRPT produces inverse magnetic catalysis in the quark condensate at high temperatures which can be understood not just as an effect of the entanglement between vacuum and magnetic contributions, but also as a resulting effect of the ultraviolet cutoff in thermal integrals.

6. Acknowledgments
This work is partially supported by Conselho Nacional de Desenvolvimento Científico e Tecnológico (CNPq), Grants No. 309598/2020-6 (R. L. S. F), No. 304518/2019-0 (S. S. A) and No. 303846/2017-8 (M. B. P); Coordenação de Aperfeiçoamento de Pessoal de Nível Superior - (CAPES-Brazil) - Finance Code 001 (W. R. T); Fundação de Amparo à Pesquisa do Estado do Rio de Janeiro (FAPERJ) (T. E. R); Fundação de Amparo à Pesquisa do Estado do Rio Grande do Sul (FAPERGS), Grants Nos. 19/2551- 0000690-0 and 19/2551-0001948-3 (R. L. S. F.). The work is also part of the project Instituto Nacional de Ciência e Tecnologia - Física Nuclear e Aplicações (INCT -FNA) Grant No. 464898/2014-5.

References
[1] Avancini S S, Farias R L, Scoccola N N and Tavares W R 2019 *Phys. Rev. D* **99** 116002 (*Preprint* 1904.02730)

[2] Avancini S S, Farias R L S, Pinto M B, Restrepo T E and Tavares W R 2021 *Phys. Rev. D* **103** 056009 (*Preprint* 2008.10720)

[3] Fukushima K 2004 *Phys. Lett. B* **591** 277–284 (*Preprint* hep-ph/0310121)

[4] Ratti C, Thaler M A and Weise W 2006 *Phys. Rev. D* **73** 014019 (*Preprint* hep-ph/0506234)

[5] Ratti C, Roessner S, Thaler M and Weise W 2007 *Eur. Phys. J. C* **49** 213–217 (*Preprint* hep-ph/0609218)

[6] Schwinger J S 1951 *Phys. Rev.* **82** 664–679

[7] Endrődi G and Markó G 2019 *JHEP* **08** 036 (*Preprint* 1905.02103)

[8] Bali G, Bruckmann F, Endrődi G, Fodor Z, Katz S and Schäfer A 2012 *Phys. Rev. D* **86** 071502 (*Preprint* 1206.4205)

[9] Tavares W R, Farias R L S, Avancini S S, Timóteo V S, Pinto M B and Krein G a 2021 *Eur. Phys. J. A* **57** 278 (*Preprint* 2104.11117)

[10] Bali G, Bruckmann F, Endrődi G, Gruber F and Schäefer A 2013 *JHEP* **04** 130 (*Preprint* 1303.1328)